Biochemistry and Biophysics Reports 39 (2024) 101807

Contents lists available at ScienceDirect

Biochemistry and Biophysics Reports

journal homepage: www.elsevier.com/locate/bbrep

Human Antigen R -mediated modulation of Transforming Growth Factor Beta 1 expression in retinal pathological milieu

Sruthi Priya Mohan [a,b], Hemavathy Nagarajan [c], Umashankar Vetrivel [d], Sharada Ramasubramanyan [a,*]

[a] R.S. Mehta Jain Department of Biochemistry and Cell Biology, KBIRVO, Vision Research Foundation, Chennai, India
[b] School of Chemical and Biotechnology, SASTRA Deemed to be University, Thanjavur, India
[c] Centre for Bioinformatics, KBIRVO, Vision Research Foundation, Chennai, India
[d] Virology & Biotechnology/Bioinformatics Division, ICMR-National Institute for Research in Tuberculosis, Chennai, India

ARTICLE INFO

Keywords:
Post-transcriptional regulation
Human Antigen R
Hypoxia
TGFβ1
Molecular docking
Molecular dynamics

ABSTRACT

The fate and stability of messenger RNA (mRNA), from transcription to degradation is regulated by a dynamic shuttle of epigenetic modifications and RNA binding proteins in maintaining healthy cellular homeostasis and disease development. While Transforming Growth Factor Beta 1 (TGFβ1) has been implicated as a key regulator for diabetic retinopathy, a microvascular complication of diabetes, the RNA binding proteins post-transcriptionally regulating its expression remain unreported in the ocular context. Further, dysfunction of TGFβ1 signalling is also strongly associated with angiogenesis, inflammatory responses and tissue fibrosis in many eye conditions leading to vision loss. In this study, computational and molecular simulations were initially carried out to identify Human Antigen R (HuR) binding sites in *TGFβ1* mRNA and predict the structural stability of these RNA-protein interactions. These findings were further validated through *in vitro* experiments utilizing Cobalt Chloride ($CoCl_2$) as a hypoxia mimetic agent in human retinal microvascular endothelial cells (HRMVEC). *In silico* analysis revealed that HuR preferentially binds to the 5′-UTR of *TGFβ1* and displayed more stable interaction than the 3′UTR. Consistent with *in silico* analysis, RNA immunoprecipitation demonstrated a robust association between HuR and *TGFβ1* mRNA specifically under hypoxic conditions. Further, silencing of HuR significantly reduced TGFβ1 protein expression upon $CoCl_2$ treatment. Thus, for the first time in ocular pathological milieu, direct evidence of HuR- *TGFβ1* mRNA interaction under conditions of hypoxia has been reported in this study providing valuable insights into RNA binding proteins as therapeutic targets for ocular diseases associated with TGFβ1 dysregulation.

1. Introduction

As the burden of diabetes mellitus (DM) as a global epidemic is on a sharp rise [1], intraocular complications can be seen in one-third of diabetic patients with an annual incidence of diabetic retinopathy (DR) ranging from 2.2 to 12.7 % [2] and is one of the leading causes of vision loss in the elderly [3]. The pathological angiogenic switch in DR is triggered mainly under conditions of hypoxia initiated by stabilization of Hypoxia-inducible factor-1α (HIF-1α), which then pilots the up-regulation of several core angiogenic proteins such as vascular endothelial growth factor (VEGF) in promoting abnormal proliferation of retinal blood vessels [4]. The current modality of treatment revolves around anti-VEGF therapies, however with growing concerns about its cost, safety, and efficacy [5–8]. In recent years, RNA binding proteins

Abbreviations: mRNA, messenger Ribose nucleic acid; MMP9, Matrix Metallopeptidase 9; COX2, Cyclooxygenase-2; CNTF, Ciliary Neurotrophic Factor; bFGF, basic Fibroblast Growth Factor; NCBI, National Center for Biotechnology Information; DMSO, Dimethyl sulfoxide; cDNA, complementary Deoxyribose nucleic acid; FBS, Fetal Bovine Serum; rRNA, ribosomal RNA; MTT, 3-(4,5-Dimethylthiazol-2-yl)-2,5-Diphenyltetrazolium Bromide; siRNA, silencing RNA; PVDF, Polyvinylidene fluoride; BSA, Bovine Serum Albumin; HEPES, 4-(2-hydroxyethyl)-1-piperazineethanesulfonic acid; KCl, Potassium Chloride; $MgCl_2$, Magnesium Chloride; DTT, Dithiothreitol; NP-40, Nonidet P-40; IgG, Immunoglobulin G; PCR, Polymerase Chain Reaction; ANOVA, Analysis of Variance; RRM, RNA Recognition Motifs; vdW, van der Waals; H-bond, Hydrogen bond.

* Corresponding author. R.S. Mehta Jain Department of Biochemistry and Cell Biology, KBIRVO, Vision Research Foundation, No. 41 (old 18), College Road, Chennai, 600 006, Tamil Nadu, India.
E-mail address: drsharada@snmail.org (S. Ramasubramanyan).

https://doi.org/10.1016/j.bbrep.2024.101807
Received 8 May 2024; Received in revised form 27 July 2024; Accepted 2 August 2024

(RBPs) are emerging as master regulators for diabetes and its related complications and therefore, open a new class of potential therapeutic targets for their treatment [9,10].

Of particular interest is Human Antigen R (HuR) that regulates key cellular processes including cell proliferation, apoptosis, mRNA trafficking, and protein translation ([11]; J. [12]). HuR binds to adenine- and uridine-rich elements (ARE) in the 3′-untranslated region (UTR) of target mRNAs and regulate their stability and translation. Most importantly, HuR bound to *VEGF* at a 40bp RNA element sequence at the 3′UTR [13] and this interaction was also observed in HeLa cells treated with a $CoCl_2$ by a pull-down assay to identify RNA-binding partners for *VEGF* mRNA [14]. Additionally, the other angiogenic molecules that are directly regulated by HuR include *HIF1α*, *COX2*, and *MMP9* ([15,16]; H. [17]) indicating a pivotal role of HuR in the molecular pathophysiology of DR. Indeed, in diabetic rats, the signalling cascade involving Protein Kinase C beta (PKCβ) and activation of HuR protein led to enhanced VEGF expression in the retina [18]. Delivery of HuR siRNA using lipopolyplexes (LPPs) into the eye significantly lowered the VEGF levels in streptozotocin (STZ)-induced diabetic rats, highlighting the therapeutic potential of regulating RBPs in combating pathological angiogenesis and associated vascular remodelling in DR [19,20]

Transforming Growth Factor β (TGF β) signalling is yet another perpetuator of DR, wherein increased TGFβ1 levels have been reported in both aqueous[21] and vitreous humor of DR patients [22,23]; TGFβ lead to increased vascular permeability by decreasing the expression levels of VE-Cadherin and Claudin 5 [24]; and TGFβ induces expression of Connective Tissue Growth Factor (CTGF) thereby regulating angio-fibrotic switch in late proliferative diabetic retinopathy (PDR) [25–27]. The therapeutic efficacy of the anti-VEGF drug, Bevacizumab is thwarted by sub-retinal fibrosis that develops in a significant number of patients with up-regulated levels of pro-fibrotic factors such as CTGF, TGFβ2, CNTF, and bFGF [28–30]. While TGFβ downstream signalling has been well characterized, the RBPs including HuR that exert their influence in its expression, particularly in association with ocular pathology remains elusive. Gene expression analysis as a quantitative measure holds key information on the regulatory networks, epigenetic regulation and translation of proteins involved in disease pathogenesis [31]. Advancement in computational and molecular technologies such as cross-linked and immunoprecipitation (CLIP) (protein-centric) and RNA affinity pull down followed by mass-spectrometric analysis (RNA-centric), allows for investigating regulation of gene expression by RBPs and its influence on disease progression [32].

Understanding the structural dynamics of RBP-RNA binding interface in the last few years has been instrumental in developing novel therapeutic moieties targeting the interaction motif. Thus, the primary objective of this study was to capture if HuR can bind and post-transcriptionally regulate *TGFβ1* mRNA expression in retinal endothelial cells under hypoxic conditions. Through *in silico* and *in vitro* approaches, it is observed that HuR could specifically bind to *TGFβ1* mRNA and its protein expression significantly down-regulated upon HuR silencing. This is the first study in an ocular context to investigate the RBP-TGFβ1 signaling axis and also report direct binding and regulation of TGFβ1 expression by HuR.

2. Materials and methods

2.1. In silico analysis of HuR-TGFβ1 interaction motifs

The *TGFβ1* mRNA sequence was retrieved from NCBI (NM_000660.7) and subjected to HuR binding site prediction using RBPmap (http://rbpmap.technion.ac.il/index.html) [33] and BRIO (http://brio.bio.uniroma2.it/) [34] respectively. Amongst the sequences, the HuR binding motif sequences spanning the 5′UTR and 3′UTR of *TGFβ1* were considered for both secondary and tertiary structure prediction using RNAfold [35] and RNA composer [36], respectively. Molecular docking of protein-RNA complexes was performed for the modelled RNA structures with HuR (PDB ID: 4ED5_ChainA) (J. [12]) using HADDOCK 2.2 [37]. Further, the docked protein-RNA complexes (best docking score) were analyzed for MMGBSA using the PRIME module of the Schrodinger suite [38,39], while the interaction analysis was performed using NUCPLOT [40] and PLIP [41].

Molecular dynamics (MD) simulation of the docked protein-RNA complexes was performed using GROMACS v2021 with CHARMM c36m as the force field. Before the simulation, the complexes were preprocessed using the Input generator-solution builder module of CHARMM-GUI [42] to generate the input files for the molecular dynamics simulation. The net charge of the system was kept neutral by adding counter ions. The system was solvated using TIP3P water molecules in a cubic box in which the edges of the protein and the solvated system will not be closer than 10 Å. Simulations are performed under periodic boundary conditions (PBC) and with the Particle Mesh Ewald (PME) method for long-range electrostatic interactions. The van der Waals interactions are smoothly switched off at 12 Å. The solvated system was minimized for 1000 steps to remove the contact clashes (atomic) in the system. Followed by energy minimization, and equilibration, the production runs were performed with an integration time-step of 2 fs (fs), and all the bond lengths involving hydrogen atoms were fixed using the SHAKE algorithm. The system was equilibrated using an NPT ensemble at 1 atm pressure and 310 K temperature with constraints and finally, MD production simulations were carried out for 200ns without any constraints and the trajectory was saved for every 10 ps. The resulting MD trajectories of the complexes were analyzed for plotting root mean square deviation (RMSD) and root mean square fluctuations (RMSF), inter-hydrogen bond interactions within the systems through its entire trajectories.

2.2. Cell culture and treatment conditions

Primary Human Retinal Microvascular Endothelial Cells (HRMVEC; # ACBRI 181) were procured from Cell Systems (Kirkland, USA) and cultured in Endothelial Growth Medium-2 (EGM-2, Lonza, Switzerland) in a humidified incubator at 37 °C with 5 % CO_2. For all experimental conditions, passage 6–8 cells were serum starved overnight in Endothelial Basal Medium (EBM) with 1 % FBS and treated with 0–200 μM of $CoCl_2$ (Sigma).

2.3. Silencing of HuR

Silencer select validated siRNAs for HuR (s4610) and negative control (4404021) were purchased from Thermo Fisher Scientific (Waltham, MA) and transfected into HRMVEC using Lipofectamine RNAiMAX (Life Technologies, Carlsbad, CA) for 24 h. The transfected cells were subsequently treated for 24 h using $CoCl_2$ for hypoxia induction and expression analysis. Cell viability was determined using MTT assay and performed as described previously [43,44].

2.4. Gene expression analysis

Total RNA was extracted from the cells using Trizol (Ambion) and converted to cDNA using the iSCRIPT cDNA synthesis kit (Bio-rad, USA). Using pre-designed primers (Supplementary Table S3), the relative expression of each target gene was normalized to *18s rRNA* and fold change values were calculated using the $2^{-\Delta\Delta}$Ct method.

2.5. Western blotting

Total cell lysates were prepared using (RIPA) lysis buffer (150 mM sodium chloride, 0.1 % TritonX-100, 0.5 % sodium deoxycholate, 0.1 % SDS (sodium dodecyl sulfate) 50 mM Tris, pH 8.0) with protease inhibitors and phosphatase inhibitor cocktail (Roche). 50 μg of protein was separated on 8–15 % SDS-PAGE gels and transferred to PVDF membrane (GE Healthcare, UK). The membranes were blocked for 1 h

and immuno-blotted using commercially available antibodies and chemi-luminescence method of detection. Primary antibodies include Anti-HIF1α (Santacruz Biotechnology, USA), Anti-HuR (Santacruz Biotechnology, USA), Anti- TGFβ1 (Cell signalling technologies) and Anti-β-actin (Santacruz Biotechnology, USA). Images were captured on a FluorChem FC3 (ProteinSimple, USA) and quantification done using ImageJ software.

2.6. RNA immunoprecipitation (RIP)

$5*10^7$ cells were lysed in RIP lysis buffer (10 mM HEPES pH-8, 40 mM KCl, 3 mM $MgCl_2$, 5 % glycerol, 2 mM DTT, and 0.5%NP-40) along with Proteinase Inhibitor cocktail (Roche) and RNAse inhibitors (Ambion). 10 % of the lysate was removed as input and the remaining lysate was incubated with magnetic beads conjugated with anti-HuR antibody or control IgG overnight at 4 °C. The beads were washed 5 times with NT-2 buffer (50 mM Tris pH:7.4, 150 mM NaCl, 1 mM $MgCl_2$, and 0.05 % NP-40) and processed for RNA isolation using the Trizol method. qPCR was performed for the target genes and fold enrichment was calculated as follows. ΔCt [normalized RIP] = Ct [RIP] – (Ct [Input] – Log2 (Input Dilution Factor)) where Input Dilution Factor = (fraction of the input RNA saved). % Input = 2(-ΔCt [normalized RIP]). ΔΔCt [RIP/IgG] = ΔCt [normalized RIP] – ΔCt [normalized IgG] and Fold Enrichment = 2 (-ΔΔCt [RIP/IgG])

2.7. RNA stability assay

To HRMVEC treated with $CoCl_2$ for 24 h, 5 μg/ml of Actinomycin D (Sigma) was added to measure mRNA decay over varying time points at 0, 2 and 4 h following treatment. RNA was extracted by trizol method and by qPCR, the mRNA abundance was calculated as follows.

ΔCt = (Average Ct of each time point - Average Ct of t = 0).

Relative mRNA abundance = 2(-ΔCt).

The mRNA decay rate was determined by non-linear regression curve fitting (one-phase decay) using GraphPad Prism.

2.8. Statistical analysis

Data were presented as mean ± S.E.M. and the statistical significance between groups was analyzed using GraphPad Prism5 software (GraphPad Software, Inc., San Diego, CA, USA). Student's *t*-test was used for the comparison of parameters between two groups and one-way ANOVA was used for the comparison of parameters between more than two groups. *P*-value of <0.05 was considered to be significant. For all tests, three levels of significance (*$P < 0.05$, **$P < 0.01$, ***$P < 0.001$) were applied.

3. Results

To determine if HuR could bind and post-transcriptionally regulate TGFβ1 expression, *in silico* analysis was carried out to identify the binding sites of HuR in the UTR regions of *TGFβ1* and model their interaction dynamics.

3.1. In silico analysis of HuR-TGFβ1 interaction

As indicated in Table 1, 5 RBP sites were identified, of which RBP sites 1 and 5 were located within the 5′UTR and 3′UTR regions of *TGFβ1* mRNA respectively. Thus, these two regions were further considered for secondary structure and tertiary structure prediction. The RBP site 1 (*TGFβ1*-5′UTR) and RBP site 5 (*TGFβ1*-3′UTR) secondary structures were predicted as shown in Fig. S1, upon which the tertiary structure was modelled for HuR binding motif including 3bp upstream and downstream of the motif as shown in Fig. 1A & B. On docking these modelled UTR segments to the HuR protein, it was observed that for *TGFβ1*-5′UTR, a total of 119 structures were clustered into 12 cluster(s) for the HuR-*TGFβ1*-5′UTR complex which represented 59.5 % of the water-refined models. In the case of the *TGFβ1*-3′UTR segment, HADDOCK clustered 130 structures into 12 cluster(s) for the HuR- *TGFβ1*-3′UTR complex representing 65.0 % of the water-refined models.

Based on the molecular docking analysis (Table 2), the *TGFβ1*-3′UTR was observed to have a better binding affinity profile with a high HADDOCK score of −121.3 ± 13.1 than the *TGFβ1*-5′UTR (−107.9 ± 13.8), in addition to the least RMSD value. Moreover, the average standard deviation (negative Z score) among clusters of HuR with *TGFβ1*-3′UTR indicates better docking among complexes *TGFβ1*-5′UTR (Table 2). Besides that, the terms electrostatic energy and van der Waals energy favored the protein-RNA complex formation, while desolvation energy hindered the same. Interestingly amongst the docked complexes, the *TGFβ1*-5′UTR was inferred to have stable interactions with HuR, with higher hydrogen bond formation (H-bonds: 28) majorly with the RRM1 domain residues and crucial T-type π-Stacking. *TGFβ1*-3′UTR showed major hydrogen bond interactions with the RRM2 domain than RRM1 domain residues, along with stable hydrophobic interactions with Lys34, and Leu35 residues of the RRM1 domain. Furthermore, the binding energy was also observed to be higher in the case of the HuR-*TGFβ1*-5′UTR complex, wherein the Coulomb, H-bond, and vdW energies have highly favored the complex formation when compared to the HuR-*TGFβ1*-3′UTR complex (see Table 3).

3.2. Stability analysis of the protein-RNA complexes

On comparative RMSD analysis (Fig. 2A) of the HuR-RNA complexes, it was observed that the *TGFβ1*-5′UTR bound HuR complex was found to be stabilized and to have maintained the least deviations (~0.6 nm)

Table 1
Prediction of the HuR binding site of *TGFβ1*.

RBP Site	Position	Occurrence	Z-score	P-value
1	679	CUGGUACCAGAUCGCGCCCAUCUAGGUUAUUUCCGUGGG AUACUGAGACACCCCCGG	1.791	3.66e-02
2	1460	UGCUGGCACCCAGCGACUCGCCAGAGUGGUUAUCUUUUG AUGUCACCGGAGUUGUGC	2.044	2.05e-02
3	1466	CACCCAGCGACUCGCCAGAGUGGUUAUCUUUUGAUGUCA CCGGAGUUGUGCGGCAGU	2.033	2.10e-02
4	1471	AGCGACUCGCCAGAGUGGUUAUCUUUUGAUGUCACCGGA GUUGUGCGGCAGUGGUUG	2.286	1.11e-02
5	2170	CGUGCCCCAAGCCCACCUGGGGCCCCAUUAAAGAUGGAG AGAGGACUGCGGAUCUC	1.953	2.54e-02

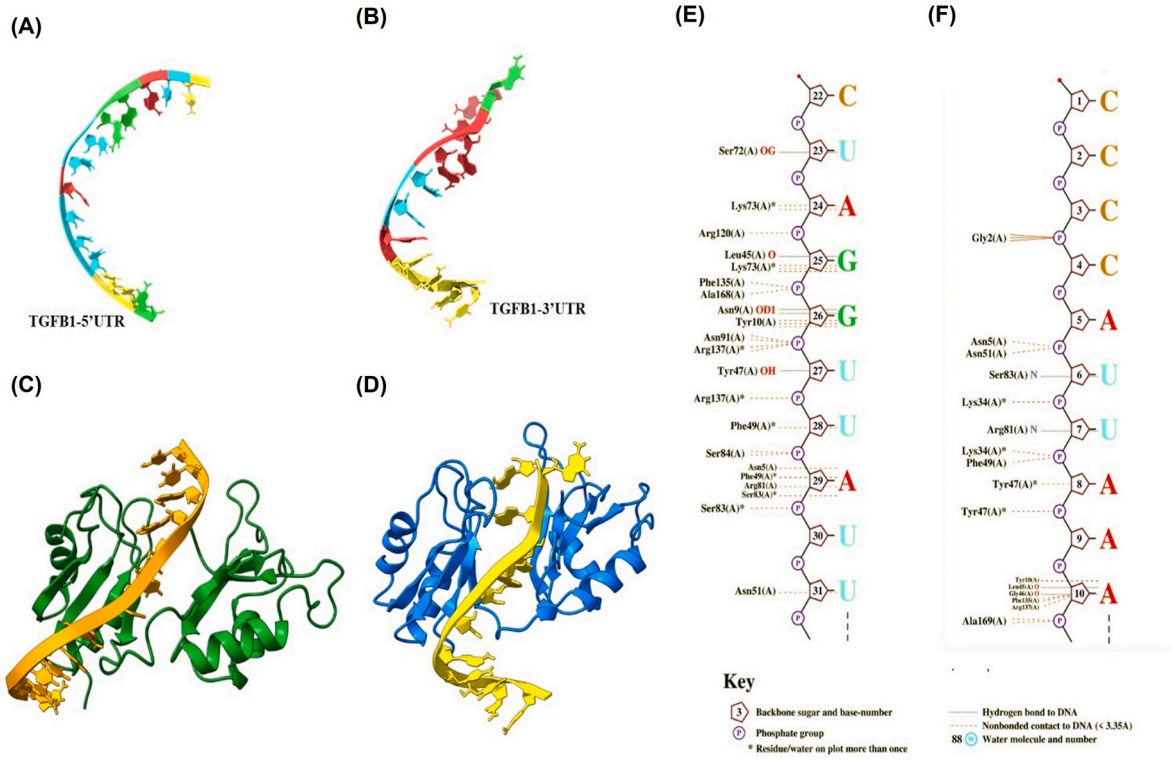

Fig. 1. Predicted three-dimensional structure of *TGFβ1* binding segments (A) 5′UTR (B) 3′UTR The docked HuR in complex with TGFβ1 segments (C) 5′UTR (D) 3′UTR. Initial interactions of the docked complexes generated by NUCPLOT (E) HuR-*TGFβ1*-5′UTR (F) HuR-*TGFβ1*-3′UTR.

Table 2
Molecular docking profiles of HuR in complex with TGFβ1 segments.

Molecular Docking Profile	HuR_*TGFβ1*-5′UTR	HuR_*TGFβ1*-3′UTR
Cluster	cluster4	cluster2
HADDOCK score [a.u]	−107.9 ± 13.8	−121.3 ± 13.1
Cluster size	15	17
RMSD from the overall lowest-energy structure (Å)	3.4 ± 2.6	1.1 ± 0.7
Van der Waals energy (kcal/mol)	−75.0 ± 6.4	−84.7 ± 8.6
Electrostatic energy (kcal/mol)	−339.1 ± 68.1	−421.2 ± 37.3
Desolvation energy (kcal/mol)	21.0 ± 4.1	33.9 ± 8.1
Restraints violation energy (kcal/mol)	138.3 ± 46.92	137.5 ± 26.59
Buried Surface Area (kcal/mol)	1755.6 ± 129.2	2137.2 ± 121.0
Z-Score	−1.6	−2

Table 3
Binding energy components from protein-RNA complex.

MMGBSA ΔG binding energy (kcal/mol)	HuR_*TGFβ1*-5′UTR	HuR_*TGFβ1*-3′UTR
Binding energy	−119.66	−111.64
Coulomb energy	−257.67	−132.82
Covalent energy	23.91	6.9
H-bond energy	−16	−9.26
Lipophilic energy	−9.39	−18.78
Solv_GB	260.12	168.96
vdW Energy	−125.84	−125.75

throughout the MD production run. Whereas the *TGFβ1*-3′UTR bound HuR complex, has tried to equilibrate at the initial 50 ns with the least RMS deviations of ~0.5 nm till 140ns, but has attained higher deviations of ~1.1 nm at 150ns, yet has stabilized in the last 40 ns. The higher deviations of the complex can be highly attributed to the higher fluctuations of the HuR in the complex with *TGFβ1*-3′UTR (Fig. 2B), which has also shown higher RMSD deviations than the *TGFβ1*-5′UTR bound state (Fig. 2D–F). From the RMSF plot (Fig. S3) of the *TGFβ1*-UTR segments, both the UTR segments have the least fluctuations. On analyzing the inter-hydrogen bond interactions of both HuR and *TGFβ1* UTR segments, 5′UTR of *TGFβ1* was observed to maintain higher hydrogen bonds (~25 H-bonds) throughout the MD than 3′UTR (~15 H-bonds). The interaction analysis of the minimum potential energy structures (Fig. 3 & Table S2) of HuR-*TGFβ1* UTR complexes (Fig. S4), *TGFβ1*-5′UTR has formed crucial π-Cation and π-Stacking (P-type stacking) with the RRM1 domain residues of HuR, while the RRM2 domain residue Arg120 has formed a π-Cation interaction with *TGFβ1*-3′UTR. Apart from these, *TGFβ1*-5′UTR has maintained stable hydrogen bonds and non-bonded interactions with HuR than the *TGFβ1*-3′UTR. Having established stable interaction of HuR to *TGFβ1* mRNA by computational analysis, *in vitro* validation was performed in HRMVEC, especially under conditions of hypoxia to direct evidence HuR binding to *TGFβ1*.

3.3. Novel binding of HuR to TGFβ1 in hypoxia-induced HMRVEC

HRMVEC treated with 200 μM of $CoCl_2$ up to 24 h did not show any cytotoxicity and significantly enhanced the expression of HIF1α protein as expected (Figure S5 &Fig. 4A). Increased TGFβ1 expression at both gene and protein level could also be observed in hypoxic HRMVEC, with *TGFβ1* mRNA stabilizing under the stress conditions (Fig. 4B, C & D). RNA immunoprecipitation assay using HuR antibody shows a novel binding of HuR to *TGFβ1* mRNA, more so in cells that are under hypoxic stress (Fig. 4E–G).

3.4. Silencing HuR reduces TGFβ1 expression

To further delineate the specific association of HuR to *TGFβ1* mRNA upon hypoxia in HRMVEC, HuR was silenced and its effect on the expression of TGFβ1 was analyzed. Using validated siRNA oligos at concentrations not toxic to the cells (Fig. S6), a significant reduction in

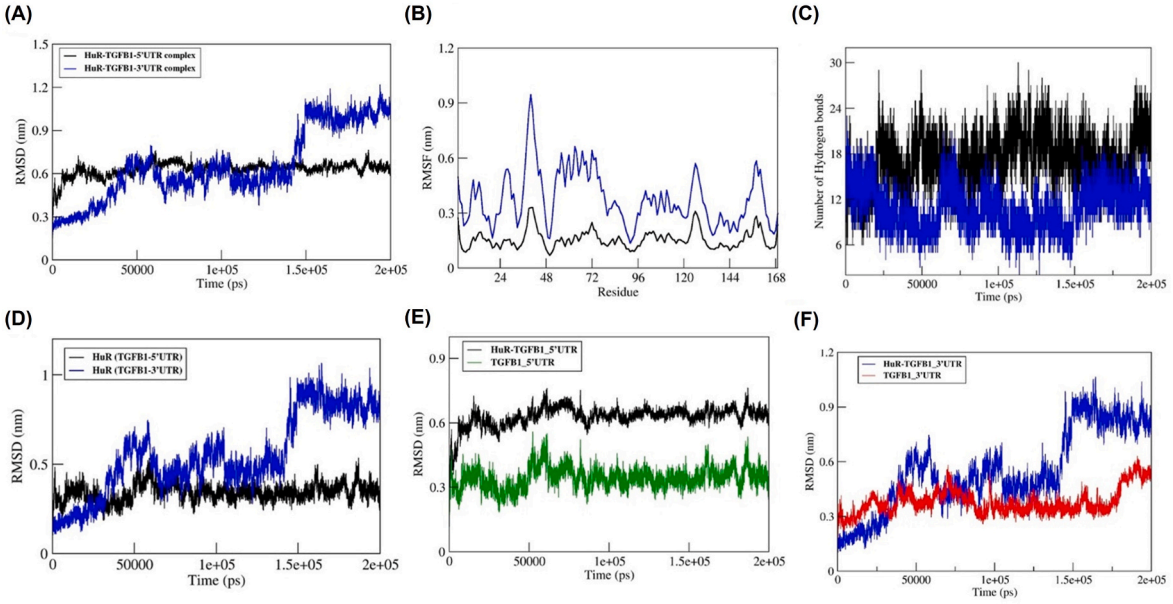

Fig. 2. Molecular dynamics simulation analysis of the complexes (A) comparative RMSD plot (B) RMSF plot of HuR (C) Inter hydrogen bond plot (D) RMSD plot of HuR bound to TGFβ1- UTRs, comparative RMSD plots of HuR and *TGFβ1*-UTRs (E) HuR-*TGFβ1*-5′UTR (F) HuR-*TGFβ1*-3′UTR.

the expression of HuR could be observed as shown in Fig. 5A. Intriguingly, in line with the hypothesis that HuR binding would affect the post-transcriptional levels of TGFβ1, HuR silencing in $CoCl_2$ treatment led to a significant decrease in protein expression of TGFβ1, but not its mRNA levels (Fig. 5C–E & B).

4. Discussion

The multi-faceted molecular networks of intraocular vascular diseases warrant that the therapeutic targets to combat ocular angiogenesis be not concentrated on molecules in individual pathways, but rather seek a convergence point for the various signaling pathways. HuR is an RNA-binding protein that is at the central dogma of angiogenesis and has been shown to modulate and influence expression levels of many pro-angiogenic factors including proteins that facilitate endothelial cell proliferation and migration. However, little is known about the influence of RNA binding proteins, particularly HuR in post-transcriptional regulation of TGFβ1 expression and its associated angio-fibrotic switch in DR which is addressed in this study.

In silico analysis revealed HuR binding sites both in the 3′UTR and the 5′ UTR regions of *TGFβ1* mRNA. Computational simulations showed that the 5′UTR segment has a higher binding affinity and stable interactions towards HuR than 3′UTR. Amongst the UTRs, only the binding of 3′UTR has induced the conformational changes of HuR, since it had major interactions with the inter-domain linker segment and RRM2 domain. Wherein the binding of 5′UTR has aided in the stability of the HuR protein with increased binding affinity. This reveals that the binding of both 5′ and 3′UTR has their respective substantial contacts towards HuR conformational changes that may be attributed to its cascade of functional mechanisms. HuR is known to predominantly bind at the 3′UTR in promoting mRNA stability and regulating the translation efficiency of target genes [16]. While the association of HuR with the 5′UTRs of some target substrates caused repression in their translation [45,46], in some it had an opposite effect leading to enhanced expression of the target proteins such as HIF1α [47,48]. Thus, the impact of HuR binding to 5′UTRs and the associated fate of the mRNAs needs further studies to understand the functional significance of RBP-mRNA interaction. But of importance is *in silico* analysis to simulate the binding of HuR to mRNA of interest assists in understanding both the structural and functional significance of the interaction, which could be targeted by competitive inhibitors as alternate therapy.

RBPs oversee and regulate post-transcriptional regulation of mRNA including their stability, transport, alternative splicing, polyadenylation and the rate of translation [49]. In fact, Neuronal Protein 3.1 (P311) is an RBP that preferentially binds to the 5′-UTR of *TGF-β1-3* mRNAs through its RRM (RNA recognition motif-like motif) domain and recruits the mRNAs to the translation machinery. This leads to enhanced translation efficiency and up-regulation of TGFβ 1–3 protein levels [50]. We report a similar observation wherein our *in silico* analysis demonstrate preferential binding of HuR to the 5-UTR of *TGF-β1* mRNA. We hypothesized that this HuR-TGFβ1 mRNA interaction would lead to stabilization of the mRNA and thereby increase the translation efficiency of TGFβ1 in HRMVECs treated with $CoCl_2$. Indeed, RIP experiments provided direct evidence for HuR binding to *TGFβ1* mRNA in hypoxia-induced retinal endothelial cells. In line with our hypothesis, silencing HuR in $CoCl_2$ treated HRMVEC cells did not alter TGFβ1 mRNA levels but rather significantly reducing its protein expression. This is further supported by previous studies wherein HuR association with *TGFβ1* mRNA led to increased secretory levels of TGFβ1 [51–53]. Interestingly, while Galban et al., reported that HuR overexpression was found to increase binding to the target mRNAs upon stress insults [47], we didn't observe any significant increase in HuR levels in HRMVECs upon $CoCl_2$ treatment (Supplementary Fig. S7) but impacted its association with the target mRNA. In this study at least, the binding affinity of HuR to target mRNAs did not depend on its protein expression levels.

This study captures for the first time in retinal cells, RBP that can post-transcriptionally regulate TGFβ1 signalling, indicating a crucial role of HuR in facilitating the angio-fibrotic switch associated with DR progression. An intricate and complex circuit of intersecting signalling pathways defines the pathogenesis of diabetes and its complications, with TGFβ signalling perpetuating the microvascular abnormalities and cellular dysfunction in DR. Thus, novel interfacial peptide inhibitors towards the HuR- *TGFβ1* mRNA interaction sites would better serve as a potential therapeutic modality not limited to DR, but also in other eye conditions with TGFβ1 dysregulation.

CRediT authorship contribution statement

Sruthi Priya Mohan: Writing – original draft, Visualization, Validation, Methodology, Investigation, Formal analysis. **Hemavathy**

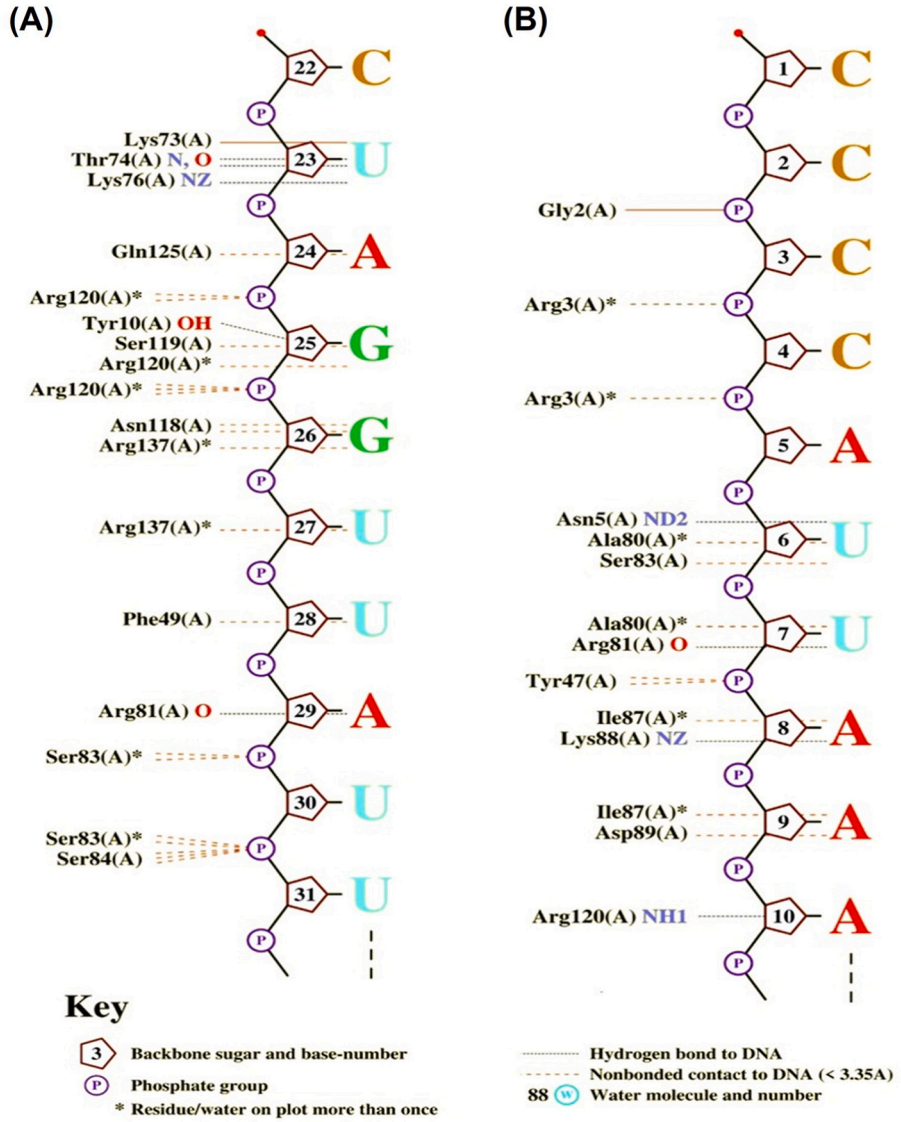

Fig. 3. Interactions of the minimum potential complexes generated by NUCPLOT (A) HuR-*TGFβ1*-5′UTR (B) HuR-*TGFβ1*-3′UTR.

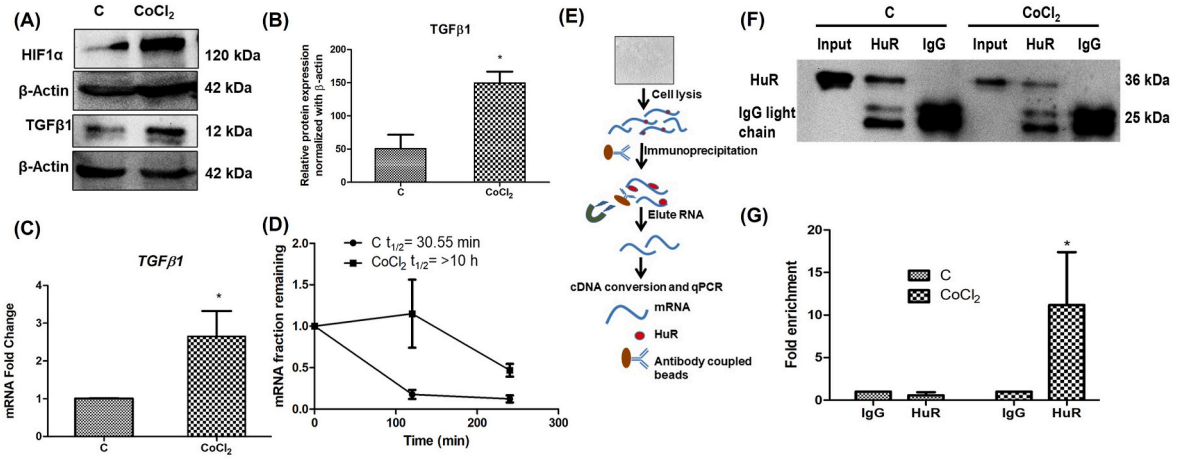

Fig. 4. HuR interaction with *TGFβ1* in hypoxic HRMVEC. HRMVEC were treated with either Control (C)/$CoCl_2$ and subjected to (A) western blotting for HIF1α and TGFβ1 with β-actin as loading control. (B) Relative protein expression of TGFβ1 normalized to β-actin. (C) qPCR for *TGFβ1* with *18s rRNA* as an internal control (D) mRNA stability assay using ActinomycinD for *TGFβ1*. (E) Schematic representation of RNA immunoprecipitation (F) western blotting for HuR in the immunoprecipitated samples [I-Input (10 %)]. (G) RNA immunoprecipitation followed by real-time PCR for *TGFβ1* (n = 3; *p < 0.05).

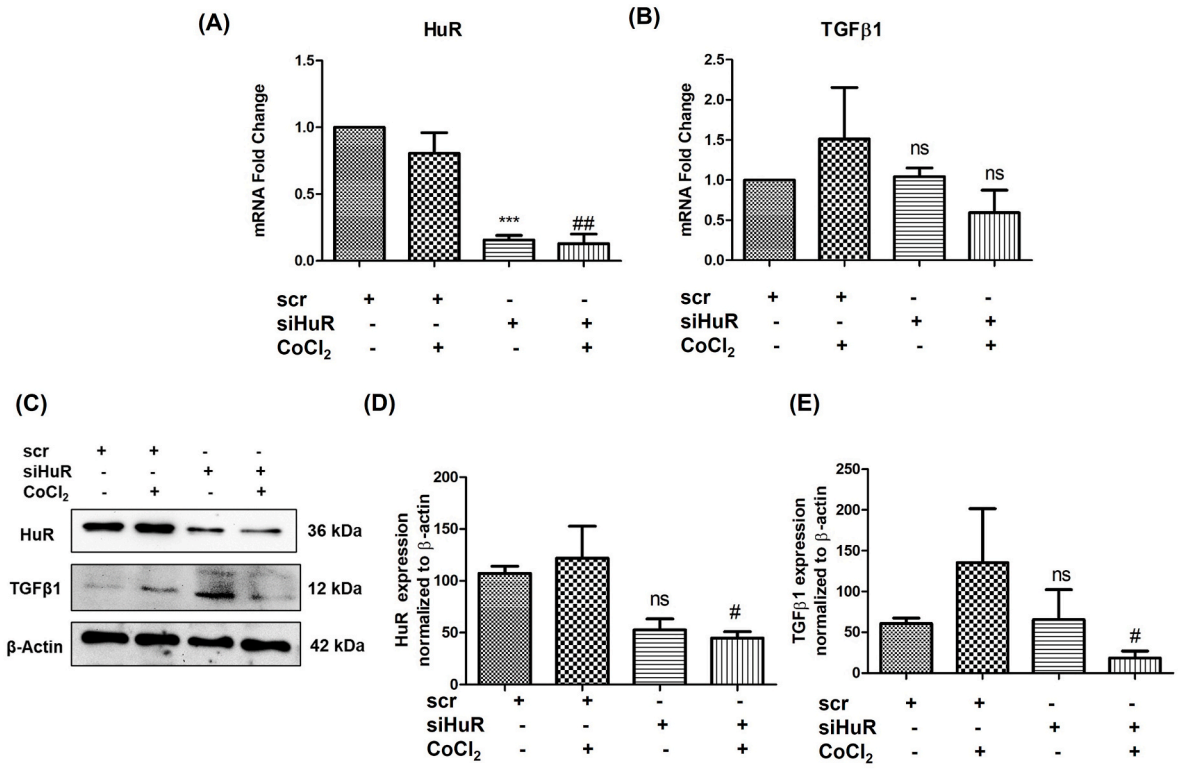

Fig. 5. siRNA experiments for HuR. HRMVEC were treated with either Scramble (Scr), Scr + $CoCl_2$, SiHuR, or SiHuR + $CoCl_2$ and subjected to (A, B) Real-time PCR for *HUR and TGFβ1* with *18s rRNA* as an internal control (n = 3; ***p < 0.001 Scr Vs SiHuR; ##p < 0.01 Scr + $CoCl_2$Vs SiHuR + $CoCl_2$, ns-not significant) (C) western blotting for HuR and TGFβ1 with β-actin as the loading control. (D & E) relative protein expression of HuR and TGFβ1 normalized to β-actin (n = 3, #p < 0.05 Scr + $CoCl_2$Vs SiHuR + $CoCl_2$, ns-not significant).

Nagarajan: Writing – original draft, Visualization, Validation, Software, Methodology, Formal analysis. **Umashankar Vetrivel:** Writing – review & editing, Visualization, Validation, Supervision, Software, Resources, Methodology, Investigation, Formal analysis, Data curation, Conceptualization. **Sharada Ramasubramanyan:** Writing – review & editing, Writing – original draft, Visualization, Validation, Supervision, Resources, Project administration, Methodology, Investigation, Funding acquisition, Formal analysis, Data curation, Conceptualization.

Declaration of competing interest

The authors declare the following financial interests/personal relationships which may be considered as potential competing interests:

Dr Sharada Ramasubramanyan reports financial support was provided by the Science and Engineering Research Board, Department of Science and Technology, India. Sruthi Priya Mohan reports financial support was provided by Indian Council of Medical Research - Senior Research Fellowship. If there are other authors, they declare that they have no known competing financial interests or personal relationships that could have appeared to influence the work reported in this paper.

5. Acknowledgments

This work was supported by the Science and Engineering Research Board, Department of Science and Technology, India [ECRA- ECR/2016/001729] and the Indian Council of Medical Research (ICMR) [2020–6636 CMB/BMS].

Appendix A. Supplementary data

Supplementary data to this article can be found online at https://doi.org/10.1016/j.bbrep.2024.101807.

References

[1] K. Ogurtsova, J.D. da Rocha Fernandes, Y. Huang, U. Linnenkamp, L. Guariguata, N.H. Cho, L.E. Makaroff, IDF Diabetes Atlas: global estimates for the prevalence of diabetes for 2015 and 2040, Diabetes Res. Clin. Pract. 128 (2017) 40–50, https://doi.org/10.1016/j.diabres.2017.03.024.

[2] C. Sabanayagam, R. Banu, M.L. Chee, R. Lee, Y.X. Wang, G. Tan, T.Y. Wong, Incidence and progression of diabetic retinopathy: a systematic review, Lancet Diabetes Endocrinol. (2018), https://doi.org/10.1016/S2213-8587(18)30128-1.

[3] K.Y. Lin, W.H. Hsih, Y.B. Lin, C.Y. Wen, T.J. Chang, Update in the epidemiology, risk factors, screening, and treatment of diabetic retinopathy, J Diabetes Investig 12 (8) (2021) 1322–1325, https://doi.org/10.1111/jdi.13480.

[4] P.A. Campochiaro, Molecular pathogenesis of retinal and choroidal vascular diseases, Prog. Retin. Eye Res. 49 (2015) 67–81.

[5] F. Esen, O. Alhan, P. Kuru, O. Sahin, Safety assessment and power analyses in published anti-vascular endothelial growth factor randomized controlled trials, Am. J. Ophthalmol. 169 (2016) 68–72.

[6] T.Q. Kwong, M. Mohamed, Anti-vascular endothelial growth factor therapies in ophthalmology: current use, controversies and the future, Br. J. Clin. Pharmacol. 78 (4) (2014) 699–706.

[7] B. Todorich, G. Yiu, P. Hahn, Current and investigational pharmacotherapeutic approaches for modulating retinal angiogenesis, Expert Rev Clin Pharmacol 7 (3) (2014) 375–391.

[8] P. Ventrice, C. Leporini, J.F. Aloe, E. Greco, G. Leuzzi, G. Marrazzo, V. Scorcia, Anti-vascular endothelial growth factor drugs safety and efficacy in ophthalmic diseases, J. Pharmacol. Pharmacother. 4 (Suppl 1) (2013) S38–S42.

[9] C. Tu, L. Wang, L. Wei, RNA-binding proteins in diabetic microangiopathy, J. Clin. Lab. Anal. 36 (5) (2022) e24407, https://doi.org/10.1002/jcla.24407.

[10] S. Zhang, X. Yang, M. Jiang, L. Ma, J. Hu, H.H. Zhang, Post-transcriptional control by RNA-binding proteins in diabetes and its related complications, Front. Physiol. 13 (2022) 953880, https://doi.org/10.3389/fphys.2022.953880.

[11] N. Embade, D. Fernandez-Ramos, M. Varela-Rey, N. Beraza, M. Sini, V. Gutierrez de Juan, M.L. Martinez-Chantar, Murine double minute 2 regulates Hu antigen R stability in human liver and colon cancer through NEDDylation, Hepatology 55 (4) (2012) 1237–1248.

[12] J. Wang, Y. Guo, H. Chu, Y. Guan, J. Bi, B. Wang, Multiple functions of the RNA-binding protein HuR in cancer progression, treatment responses and prognosis, Int. J. Mol. Sci. 14 (5) (2013) 10015–10041, https://doi.org/10.3390/ijms140510015.

[13] I. Goldberg-Cohen, H. Furneauxb, A.P. Levy, A 40-bp RNA element that mediates stabilization of vascular endothelial growth factor mRNA by HuR, J. Biol. Chem. 277 (16) (2002) 13635–13640, https://doi.org/10.1074/jbc.M108703200.

[14] C. Osera, J.L. Martindale, M. Amadio, J. Kim, X. Yang, C.A. Moad, A. Pascale, Induction of VEGFA mRNA translation by CoCl2 mediated by HuR, RNA Biol. 12 (10) (2015) 1121–1130.
[15] R. Dong, G.D. Yang, N.A. Luo, Y.Q. Qu, HuR: a promising therapeutic target for angiogenesis, Gland Surg. 3 (3) (2014) 203–206.
[16] M.R. Smith, G. Costa, RNA-binding proteins and translation control in angiogenesis, FEBS J. 289 (24) (2022) 7788–7809, https://doi.org/10.1111/febs.16286.
[17] H. Wang, N. Ding, J. Guo, J. Xia, Y. Ruan, Dysregulation of TTP and HuR plays an important role in cancers, Tumour Biol 37 (2016) 14451–14461.
[18] M. Amadio, C. Bucolo, G.M. Leggio, F. Drago, S. Govoni, A. Pascale, The PKCbeta/HuR/VEGF pathway in diabetic retinopathy, Biochem. Pharmacol. 80 (8) (2010) 1230–1237, https://doi.org/10.1016/j.bcp.2010.06.033.
[19] M. Amadio, A. Pascale, S. Cupri, R. Pignatello, C. Osera, D.A. V, C. Bucolo, Nanosystems based on siRNA silencing HuR expression counteract diabetic retinopathy in rat, Pharmacol. Res. 111 (2016) 713–720, https://doi.org/10.1016/j.phrs.2016.07.042.
[20] S. Supe, A. Upadhya, S. Tripathi, V. Dighe, K. Singh, Liposome-polyethylenimine complexes for the effective delivery of HuR siRNA in the treatment of diabetic retinopathy, Drug Deliv Transl Res 13 (6) (2023) 1675–1698, https://doi.org/10.1007/s13346-022-01281-9.
[21] L. Saucedo, I.B. Pfister, S. Zandi, C. Gerhardt, J.G. Garweg, Ocular TGF-beta, matrix metalloproteinases, and TIMP-1 increase with the development and progression of diabetic retinopathy in type 2 diabetes mellitus, Mediators Inflamm 2021 (2021) 9811361, https://doi.org/10.1155/2021/9811361.
[22] Y. Dai, Z. Wu, F. Wang, Z. Zhang, M. Yu, Identification of chemokines and growth factors in proliferative diabetic retinopathy vitreous, BioMed Res. Int. 2014 (2014) 486386, https://doi.org/10.1155/2014/486386.
[23] A.K. McAuley, P.G. Sanfilippo, A.W. Hewitt, H. Liang, E. Lamoureux, J.J. Wang, P. P. Connell, Vitreous biomarkers in diabetic retinopathy: a systematic review and meta-analysis, J Diabetes Complications 28 (3) (2014) 419–425, https://doi.org/10.1016/j.jdiacomp.2013.09.010.
[24] W. Shen, S. Li, S.H. Chung, L. Zhu, J. Stayt, T. Su, M.C. Gillies, Tyrosine phosphorylation of VE-cadherin and claudin-5 is associated with TGF-beta1-induced permeability of centrally derived vascular endothelium, Eur. J. Cell Biol. 90 (4) (2011) 323–332, https://doi.org/10.1016/j.ejcb.2010.10.013.
[25] D.R. Hinton, S. He, M.L. Jin, E. Barron, S.J. Ryan, Novel growth factors involved in the pathogenesis of proliferative vitreoretinopathy, Eye (Lond) 16 (4) (2002) 422–428, https://doi.org/10.1038/sj.eye.6700190.
[26] E.J. Kuiper, F.A. Van Nieuwenhoven, M.D. de Smet, J.C. van Meurs, M.W. Tanck, N. Oliver, R.O. Schlingemann, The angio-fibrotic switch of VEGF and CTGF in proliferative diabetic retinopathy, PLoS One 3 (7) (2008) e2675, https://doi.org/10.1371/journal.pone.0002675.
[27] S.E. Wheeler, N.Y. Lee, Emerging roles of transforming growth factor beta signaling in diabetic retinopathy, J. Cell. Physiol. 232 (3) (2017) 486–489, https://doi.org/10.1002/jcp.25506.
[28] J.K. Li, F. Wei, X.H. Jin, Y.M. Dai, H.S. Cui, Y.M. Li, Changes in vitreous VEGF, bFGF and fibrosis in proliferative diabetic retinopathy after intravitreal bevacizumab, Int. J. Ophthalmol. 8 (6) (2015) 1202–1206, https://doi.org/10.3980/j.issn.2222-3959.2015.06.22.
[29] S. Roy, S. Amin, S. Roy, Retinal fibrosis in diabetic retinopathy, Exp. Eye Res. 142 (2016) 71–75, https://doi.org/10.1016/j.exer.2015.04.004.
[30] M. Zhang, S. Chu, F. Zeng, H. Xu, Bevacizumab modulates the process of fibrosis in vitro, Clin. Exp. Ophthalmol. 43 (2) (2015) 173–179, https://doi.org/10.1111/ceo.12374.
[31] S. Ulhas, A.C.L. Kadam, Schulz Burkhard, Joseph Irudayaraj, Gene expression analysis using conventional and imaging methods, DNA and RNA Nanobiotechnologies in Medicine: Diagnosis and Treatment of Diseases. RNA Technologies (2013), https://doi.org/10.1007/978-3-642-36853-0_6.
[32] M. Dodel, G. Guiducci, M. Dermit, S. Krishnamurthy, E.L. Alard, F. Capraro, F. K. Mardakheh, TREX reveals proteins that bind to specific RNA regions in living cells, Nat. Methods 21 (3) (2024) 423–434, https://doi.org/10.1038/s41592-024-02181-1.
[33] I. Paz, I. Kosti, M. Ares Jr., M. Cline, Y. Mandel-Gutfreund, RBPmap: a web server for mapping binding sites of RNA-binding proteins, Nucleic Acids Res. 42 (Web Server issue) (2014) W361–W367, https://doi.org/10.1093/nar/gku406.
[34] A. Guarracino, G. Pepe, F. Ballesio, M. Adinolfi, M. Pietrosanto, E. Sangiovanni, M. Helmer-Citterich, BRIO: a web server for RNA sequence and structure motif scan, Nucleic Acids Res. 49 (W1) (2021) W67–W71, https://doi.org/10.1093/nar/gkab400.
[35] A.R. Gruber, R. Lorenz, S.H. Bernhart, R. Neubock, I.L. Hofacker, The Vienna RNA websuite, Nucleic Acids Res. 36 (Web Server issue) (2008) W70–W74, https://doi.org/10.1093/nar/gkn188.
[36] M. Antczak, M. Popenda, T. Zok, J. Sarzynska, T. Ratajczak, K. Tomczyk, M. Szachniuk, New functionality of RNAComposer: an application to shape the axis of miR160 precursor structure, Acta Biochim. Pol. 63 (4) (2016) 737–744, https://doi.org/10.18388/abp.2016_1329.
[37] G.C.P. van Zundert, J. Rodrigues, M. Trellet, C. Schmitz, P.L. Kastritis, E. Karaca, A. Bonvin, The HADDOCK2.2 web server: user-friendly integrative modeling of biomolecular complexes, J. Mol. Biol. 428 (4) (2016) 720–725, https://doi.org/10.1016/j.jmb.2015.09.014.
[38] X. He, V.H. Man, B. Ji, X.Q. Xie, J. Wang, Calculate protein-ligand binding affinities with the extended linear interaction energy method: application on the Cathepsin S set in the D3R Grand Challenge 3, J. Comput. Aided Mol. Des. 33 (1) (2019) 105–117, https://doi.org/10.1007/s10822-018-0162-6.
[39] M.P. Jacobson, D.L. Pincus, C.S. Rapp, T.J. Day, B. Honig, D.E. Shaw, R.A. Friesner, A hierarchical approach to all-atom protein loop prediction, Proteins 55 (2) (2004) 351–367, https://doi.org/10.1002/prot.10613.
[40] N.M. Luscombe, R.A. Laskowski, J.M. Thornton, NUCPLOT: a program to generate schematic diagrams of protein-nucleic acid interactions, Nucleic Acids Res. 25 (24) (1997) 4940–4945, https://doi.org/10.1093/nar/25.24.4940.
[41] S. Salentin, S. Schreiber, V.J. Haupt, M.F. Adasme, M. Schroeder, PLIP: fully automated protein-ligand interaction profiler, Nucleic Acids Res. 43 (W1) (2015) W443–W447, https://doi.org/10.1093/nar/gkv315.
[42] J. Lee, X. Cheng, J.M. Swails, M.S. Yeom, P.K. Eastman, J.A. Lemkul, W. Im, CHARMM-GUI input generator for NAMD, GROMACS, AMBER, OpenMM, and CHARMM/OpenMM simulations using the CHARMM36 additive force field, J Chem Theory Comput 12 (1) (2016) 405–413, https://doi.org/10.1021/acs.jctc.5b00935.
[43] R.N. Nareshkumar, K.N. Sulochana, K. Coral, Inhibition of angiogenesis in endothelial cells by Human Lysyl oxidase propeptide, Sci. Rep. 8 (1) (2018) 10426, https://doi.org/10.1038/s41598-018-28745-8.
[44] R. Ramya, K. Coral, S.R. Bharathidevi, RAGE silencing deters CML-AGE induced inflammation and TLR4 expression in endothelial cells, Exp. Eye Res. 206 (2021) 108519, https://doi.org/10.1016/j.exer.2021.108519.
[45] D.M. Pineda, D.W. Rittenhouse, C.C. Valley, J.A. Cozzitorto, R.A. Burkhart, B. Leiby, J.R. Brody, HuR's post-transcriptional regulation of Death Receptor 5 in pancreatic cancer cells, Cancer Biol. Ther. 13 (10) (2012) 946–955, https://doi.org/10.4161/cbt.20952.
[46] C. Winkler, A. Doller, G. Imre, A. Badawi, T. Schmid, S. Schulz, W. Eberhardt, Attenuation of the ELAV1-like protein HuR sensitizes adenocarcinoma cells to the intrinsic apoptotic pathway by increasing the translation of caspase-2L, Cell Death Dis. 5 (7) (2014) e1321, https://doi.org/10.1038/cddis.2014.279.
[47] S. Galban, Y. Kuwano, R. Pullmann Jr., J.L. Martindale, H.H. Kim, A. Lal, M. Gorospe, RNA-binding proteins HuR and PTB promote the translation of hypoxia-inducible factor 1alpha, Mol. Cell Biol. 28 (1) (2008) 93–107, https://doi.org/10.1128/MCB.00973-07.
[48] L.G. Sheflin, A.P. Zou, S.W. Spaulding, Androgens regulate the binding of endogenous HuR to the AU-rich 3'UTRs of HIF-1alpha and EGF mRNA, Biochem. Biophys. Res. Commun. 322 (2) (2004) 644–651, https://doi.org/10.1016/j.bbrc.2004.07.173.
[49] P. Zhang, W. Wu, C. Ma, C. Du, Y. Huang, H. Xu, Y. Xu, RNA-binding proteins in the regulation of adipogenesis and adipose function, Cells 11 (15) (2022), https://doi.org/10.3390/cells11152357.
[50] M.M. Yue, K. Lv, S.C. Meredith, J.L. Martindale, M. Gorospe, L. Schuger, Novel RNA-binding protein P311 binds eukaryotic translation initiation factor 3 subunit b (eIF3b) to promote translation of transforming growth factor beta1-3 (TGF-beta1-3), J. Biol. Chem. 289 (49) (2014) 33971–33983, https://doi.org/10.1074/jbc.M114.609495.
[51] D. Bai, Q. Gao, C. Li, L. Ge, Y. Gao, H. Wang, A conserved TGFbeta1/HuR feedback circuit regulates the fibrogenic response in fibroblasts, Cell. Signal. 24 (7) (2012) 1426–1432, https://doi.org/10.1016/j.cellsig.2012.03.003.
[52] L.C. Green, S.R. Anthony, S. Slone, L. Lanzillotta, M.L. Nieman, X. Wu, M. Tranter, Human antigen R as a therapeutic target in pathological cardiac hypertrophy, JCI Insight 4 (4) (2019), https://doi.org/10.1172/jci.insight.121541.
[53] S. Panneerdoss, V.K. Eedunuri, P. Yadav, S. Timilsina, S. Rajamanickam, S. Viswanadhapalli, M.K. Rao, Cross-talk among writers, readers, and erasers of m(6)A regulates cancer growth and progression, Sci. Adv. 4 (10) (2018) eaar8263, https://doi.org/10.1126/sciadv.aar8263.